Kent Academic Repository

Downloaded from

The version of record is available from

This document version
UNSPECIFIED

DOI for this version

Licence for this version
UNSPECIFIED

Additional information

Versions of research works

Versions of Record

Author Accepted Manuscripts

Enquiries

340-344

Proc. Eighth Eur. Soc. Glass Sci. Technol. Conf. Phys. Chem. Glasses: Eur. J. Glass Sci. Technol. B, October 2007, 48 (5), xxx-yyy

An x-ray diffraction study of the structure of Bioglass and its sol-gel analogue as a function of composition

V. FitzGerald,[1] D. M. Pickup, D. Carta, D. Greenspan[#] & R. J. Newport

School of Physical Sciences, University of Kent at Canterbury, CT2 7NH, UK
[#] NovaMin Technology Inc., 13709 Progress Blvd., suite #23 Alachua, FL 32615, USA

The FDA approved BioGlass® product is one of very few bone regenerative materials actually in clinical use, having been used in ~650,000 cases already. The BioGlass family are, in essence, melt quenched calcium silicate glasses with additional alkali and aklaline earth modifiers, of general compositions $CaO-Na_2O-P_2O_5-SiO_2$. We report herein the first high energy x-ray diffraction data on this important material in the hope of providing a more direct experimental insight into the glass structure. The structure of three compositions of melt quenched bioactive glass (45S5 (Bioglass), 55S5, and 60S5) and one composition of an analogous (i.e. it has similar structure and properties but has different elemental composition) sol-gel bioactive glass (77S5) have been investigated. There are significant changes occurring as a function of composition and of preparation method, but these may all be ascribed to the relative concentrations of the sample's constituent elements (e.g. the absence of Na as a network modifier in the sol-gel sample and the counter effect of the presence of –OH, and the overall variation of the Si-associated features as the relative SiO_2 fraction alters). Overall, the underlying network structure is seen to be comparable in all samples.

1. Introduction

Average life expectancy in the western world has increased dramatically with better nutrition and improvements in medical care. To allow people to remain active, and to contribute to society for longer, the need for new materials to replace and repair worn out and damaged tissues becomes ever more important. A class of melt quenched silicate glasses, containing calcium, phosphorus and alkali metals, and having the ability to promote bone regeneration and to fuse to living bone, creating strong implants with less danger of interfacial instability than previous materials, arose from the work of Hench in the USA and in the UK.[1–6] This is now produced as Bioglass and sold under the brand names of PerioGlas®, NovaBone® and NovaBone-C/M®.[7] The study of atomic scale structure has hitherto been limited to electron microscopy and infrared spectroscopy, together with exploratory molecular dynamics, MD, simulation. Here we present the first high energy x-ray diffraction (HEXRD) data on these compositions of bioactive glasses.

2. Experimental methods

2.1 Sample preparation
The samples of Bioglass were supplied by Novamin Technology, Alachua, FL. The samples were in granu-

Table 1. Sample characterisation on the basis of XRF, (using charge balancing to determine oxygen concentrations), and helium pycnometry

	45S5	55S5	60S5	77S5
Density/gcm⁻³ (±0·002)	2·708	2·624	2·612	2·309
Density/atoms Å⁻³	0·07761	0·07589	0·07592	0·06676
wt%				
CaO	26·9	22·2	19·6	16·0
SiO₂	46·1	55·1	60·1	80·0
P₂O₅	2·6	2·6	2·6	4·0
Na₂O	24·4	20·1	17·7	-
at% (±0·003)				
Ca	0·101	0·082	0·072	0·059
Si	0·161	0·191	0·207	0·275
P	0·004	0·004	0·004	0·006
Na	0·083	0·068	0·059	-
O	0·651	0·655	0·658	0·660

lar form, the composition and density are reported in Table 1. Composition analysis was performed using a Bruker S4 x-ray fluorescence spectrometer. Density measurements were performed using a Quantachrome multipycnometer and were based on the use of He as the probe gas. Samples 45S5, 55S5 and 60S5 are melt-quenched glasses. Sample 77S5 is a sol-gel glass.

2.2 X-ray diffraction experimental method and data analysis

The high energy x-ray diffraction (HEXRD) data were collected on Station 9.1 at the synchrotron radiation source (SRS), Daresbury Laboratory, UK. The finely

powdered samples were enclosed inside a 1 mm thick circular aluminium annulus by polyimide windows, and mounted to provide a flat plate θ:2θ sample geometry. The wavelength was set at λ=0·4875 Å, and calibrated using the K-edge of an Ag foil; this value is low enough to provide data to a high value of momentum transfer ($\hbar Q$, where Q_{max}=4πsinθ/λ~23 Å^{-1}; 2θ is the scattering angle, and λ is the wavelength of the diffracted radiation). The data were corrected using a suite of programs written in-house, but based upon the methodology of Warren.[8]

The initial stage of analysis of x-ray diffraction data from an amorphous material involves the removal of background scattering, normalisation, correction for absorption and inelastic scattering, and subtraction of the self scattering term from the scattered intensity.[9] No correction was made to account for multiple scattering since this may be shown to be negligible in high energy x-ray diffraction in cases such as this where there is low total sample attenuation. The resultant interference function, $i(Q)$, can reveal structural information by Fourier transformation to obtain the pair distribution function

$$T(r) = T^0(r) + \int_0^\infty Qi(Q)M(Q)\sin(Qr)\,\mathrm{d}(Q)$$

where $T^0(r)$=2$\pi^2 r\rho_0$ (r is the atomic separation between atoms and ρ_0 is the macroscopic number density) and $M(Q)$ is a window function necessitated by the finite maximum experimentally attainable value of Q (in the present case, a Hanning function was adopted[10]).

Structural information can be obtained from the diffraction data by simulating the Q-space data and converting the results to r-space by Fourier transformation to allow comparison with the experimentally determined correlation function, and then iterating the process.[11] The Q-space simulation is generated using the following equation

$$p(Q)_{ij} = \frac{N_{ij}w_{ij}}{c_j}\frac{\sin QR_{ij}}{QR_{ij}}\exp\left[\frac{-Q^2\sigma_{ij}^2}{2}\right]$$

where $p(Q)_{ij}$ is the pair function in reciprocal space, N_{ij}, R_{ij} and σ_{ij} are the coordination number, atomic separation and disorder parameter, respectively, of atom i with respect to j; c_j is the concentration of atom j, and w_{ij} is the associated weighting factor. The weighting factors are given by

$$w_{ij} = \frac{2c_i c_j f(Q)_i\, f(Q)_j}{f(Q)^2} \qquad \text{if } i{\neq}j$$

or

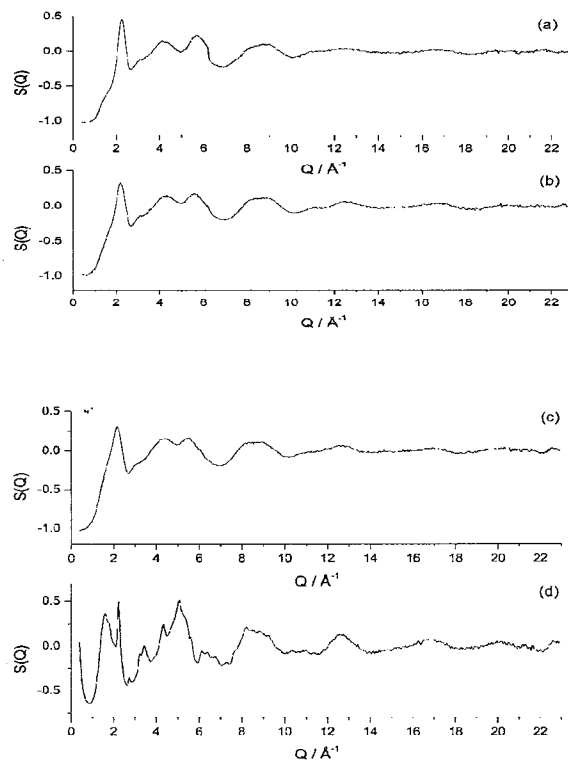$$w_{ij} = \frac{c_i^2 f(Q)_i^2}{f(Q)^2} \qquad \text{if } i{=}j$$

Figure 1. High energy x-ray diffraction data from: (a) the 45S5 Bioglass melt quenched sample: Q-space interference function S(Q) (b) the 55S5 Bioglass melt quenched sample: Q-space interference function S(Q), (c) the 60S5 Bioglass melt quenched sample: Q-space interference function S(Q), and (d) the 77S5 Bioglass sol-gel sample: Q-space interference function S(Q)

where $f(Q)$ represents the Q-dependant x-ray form factors.

3. Results

Figure 2 shows the $T(r)$ functions for three compositions of melt quenched bioactive glass and one sol-gel bioactive analogue after Fourier transformation of the experimentally derived $S(Q)$ (shown in Figure 1) into r-space, together with the simulation to the pair distribution function obtained using the method described above. The compositions and densities of samples are shown in Table 1. Three distinct features can be observed in all four cases. The peak centred around 1·6 Å is associated with the Si–O (1·61 Å) and P–O (1·43 and 1·58 Å) pairwise correlations, and the peak at ~2·5 Å is assigned to three Ca–O bond distances of 2·32, 2·5, 2·76 Å, along with the O–O nearest neighbour distance at 2·64 Å and also the Na–O distance at 2·4 Å (with the obvious exception of the sol-gel sample). Finally, the double peak centred at 3·5 Å is associated with the Si–Si second neighbour pairwise correlation (3·03 Å) and the corresponding Si–Ca, Ca–Ca correlations at 3·22, 3·5 Å,
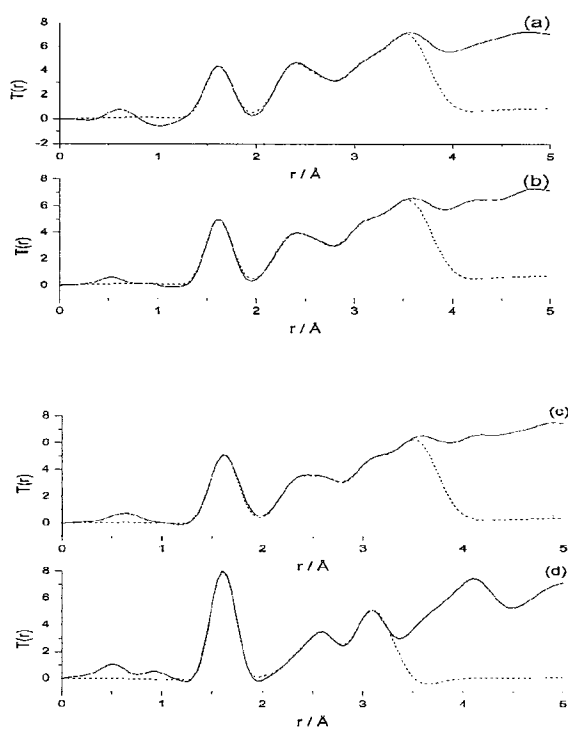
Figure 2. High energy x-ray diffraction data from: (a) the 45S5 Bioglass melt quenched sample pair distribution function, T(r), (solid line) together with fit (dashed line), (b) the 55S5 Bioglass melt quenched sample pair distribution function, T(r), (solid line) together with fit (dashed line), (c) the 60S5 Bioglass melt quenched sample pair distribution function, T(r), (solid line) together with fit (dashed line), and (d) the 77S5 Bioglass sol-gel sample pair distribution function, T(r), (solid line) together with fit (dashed line)

Table 2. Structural parameters for the Bioglass® samples obtained by fitting the high energy x-ray diffraction pair distribution functions. Note that the errors are ±0·02 Å in R, ±15% in N and ±0·01 Å in σ

Sample	Correlation	R / Å	N	σ / Å
45S5	Si–O	1·61	4·0	0·06
	Ca–O	2·29	2·3	0·07
	Na–O	2·39	6·0	0·08
	Ca–O	2·50	2·3	0·11
	O–O	2·64	4·0	0·14
	Ca–O	2·76	1·8	0·11
	Si–Si	3·03	4·4	0·11
	Si–Ca	3·22	2·8	0·16
	Ca–Ca	3·52	0·5	0·18
55S5	Si–O	1·62	3·9	0·06
	Ca–O	2·28	2·4	0·07
	Na–O	2·40	6·0	0·08
	Ca–O	2·51	2·4	0·11
	O–O	2·65	4·5	0·14
	Ca–O	2·76	1·1	0·11
	Si–Si	3·03	4·0	0·11
	Si–Ca	3·22	2·1	0·16
	Ca–Ca	3·52	0·6	0·19
60S5	Si–O	1·61	3·9	0·07
	Ca–O	2·28	2·8	0·07
	Na–O	2·39	6·2	0·07
	Ca–O	2·50	2·1	0·11
	O–O	2·64	4·6	0·10
	Ca–O	2·76	1·7	0·11
	Si–Si	3·02	4·2	0·11
	Si–Ca	3·22	2·0	0·16
	Ca–Ca	3·52	0·9	0·18
77S5	P–O	1·43	3·0	0·03
	P–O	1·58	1·0	0·03
	Si–O	1·61	4·2	0·03
	Ca–O	2·33	2·3	0·04
	Ca–O	2·49	2·6	0·07
	O–O	2·62	5·5	0·08
	Ca–O	2·79	0·6	0·12
	Si–Si	3·03	3·9	0·13
	Si–Ca	3·21	1·5	0·15
	Ca–Ca	3·50	0·2	0·14

respectively, along with contributions from Ca–P, Na–Ca and Na–Na. The assignments of the Si–O and O–O correlations are made on the basis of previous HEXRD results from metal doped sol-gel derived silicate glass,[12] and the assignment of the distances involving Ca are based on an experiment undertaken on a bioactive calcia–silica sol-gel glass using neutron diffraction with isotopic substitution.[13] The assignment of the Na–O distance is based on work by Du & Cormack.[14] The assignment of P–O distances are based on a study of vitreous P_2O_5.[15] It is evident that, on the basis of the structural parameters derived from the simulation process, given in Table 2, significant structural changes are occurring in these materials both as a function of composition and of preparation method. It is possible in all cases to simulate a Si–O peak at 1·61 Å with a coordination of ~4, although we note the fact that the coordination number is on average slightly higher than 4 as simulated. This is probably associated with residual uncertainties in sample density and composition, which will affect the

peak areas directly, and in the absence of independent data we have chosen not to scale the $T(r)$. Naturally therefore, all other simulated coordination numbers are also likely therefore to be marginally higher than they ought to be. In all samples we obtain an O–Si–O peak at ~2·64 Å however the coordination varies with Si content from ~4–6. All samples have a Si–Si distance of ~3·03 Å as expected and a coordination of ~4, however this coordination decreases as the amount of Ca increases. All samples also have a Si–Ca distance of ~3·22 Å and a coordination of 2·80 which decreases to 1·50 as Ca content decreases. The total Ca–O coordination over all three correlation distances is ~6·1, which agrees well with the results of earlier experimental[16] and molecular dynamics[17] studies on melt quenched calcium silicate glasses. All melt quenched samples showed a Na–O pair correlation peak at ~2·40 Å with a coordination of ~6, the 77S5 sol-gel glass however showed one obvious difference in the pair distribution function compared with the melt quenched samples, namely the absence of this Na–O pair correlation peak (the sol-gel sample contained no Na_2O). This can clearly be seen in Figure
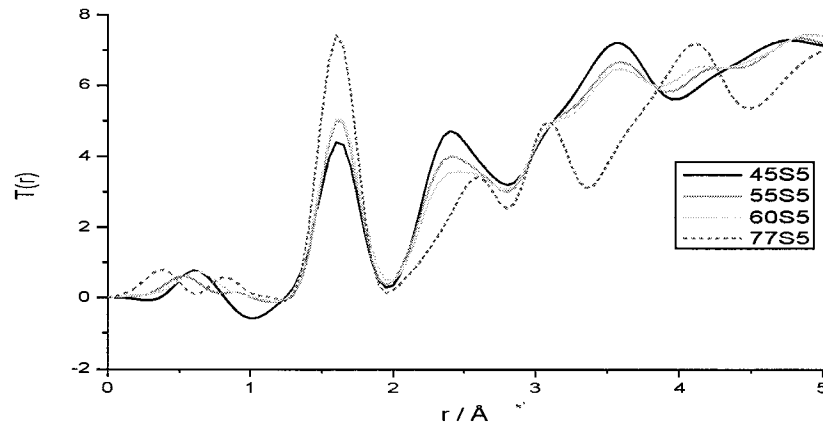
Figure 3. High energy x-ray diffraction data from: (a) the 45S5 Bioglass melt-quenched sample: pair distribution function, T(r), (solid black line), (b) the 55S5 Bioglass melt-quenched sample: pair distribution function, T(r), (solid red line) (c) the 60S5 Bioglass melt-quenched sample: pair distribution function, T(r), (solid green line), and (d) the 77S5 Bioglass sol-gel sample: pair distribution function, T(r), (dotted blue line)

3. The absence of Na is obvious and also the absence of some Ca is also apparent, along with the effect of the higher Si content.

4. Discussion

The results in Table 2 show that three pairwise correlations characteristic of the host silica network are present in the data presented here: the Si–O bond at 1·61 Å, the O–Si–O nearest neighbour distance at 2·64 Å and the Si–O–Si nearest neighbour distance at 3·03 Å. All samples exhibit a Si–O coordination number of close to four, which is as anticipated for silica-based materials.[18]

The O–Si–O coordination number would tend towards six in a fully densified silica network, but in these samples the coordination is ~4 in the 45S5 sample which has the lowest concentration of Si, whereas in the sol-gel sample, which has the highest concentration of Si the coordination is ~5·5. The results show a general trend of decreasing O–Si–O coordination number with increasing Ca and Na content suggesting Ca or Na is acting as a network modifier. The Si–O–Si coordination number should exhibit a similar trend with composition, although the errors associated with this parameter are much larger because this Si–Si first neighbour correlation is not resolved in the pair distribution functions themselves. We note here that all Si–Si coordination numbers are 4 or greater which one would not expect unless in a fully densified silica network. This is attributed to the fact that the Si–Si peak is not well resolved from overlapping correlations; furthermore, due to residual uncertainties in composition (most notably in the case of the sol-gel sample) and the effect this may have on the corrections used in data analysis, there may be a systematic error in the areas of the T(r) peaks. All the samples exhibit three Ca–O distances

with a total coordination number of between 5 and 6·5. This agrees with a previous experiment on a bioactive sol-gel glass.[13] The Na–O peaks all have a distance of ~2·40 Å and a coordination of ~6. The distance agrees with previous published data.[14] The coordination of ~6, again recalling that all coordinations will be marginally higher than they should be, agrees well with that expected for α-$Na_2Si_2O_5$, as in this material sodium coordination numbers are five and six.[19] We note that in our simulations we have a large number of partial correlation functions, and it may therefore be beneficial in a heuristic sense to combine the Ca–O and Na–O correlations with one modifier–oxygen, M–O, pseudo-correlation. Assuming a material of the generic formula $MO_x(SiO_2)_{1-x}$, parameters for the M–O correlations have been found by a weighted averaging all of the M–O correlation peaks within our T(r) simulations. These results are shown for reference purposes in Table 3. Due to and the need to employ accurate form factors for all pairwise terms in producing the simulations, it is

Table 3. Weighted average simulated parameters assuming a generic sample $MO_x(SiO_2)_{1-x}$; uncertainties are the same as those quoted in Table 2

Sample	Correlation	R / Å	N	σ / Å
45S5	Si–O	1·61	4·0	0·06
	M–O	2·49	12·4	0·19
	O–O	2·64	4·0	0·14
	Si–Si	3·03	4·4	0·11
55S5	Si–O	1·62	3·9	0·06
	M–O	2·49	11·9	0·19
	O–O	2·65	4·5	0·14
	Si–Si	3·03	4·0	0·11
60S5	Si–O	1·61	3·9	0·07
	M–O	2·49	12·8	0·18
	O–O	2·64	4·6	0·10
	Si–Si	3·02	4·2	0·11
77S5	Si–O	1·61	4·1	0·05
	M–O	2·52	5·6	0·17
	O–O	2·62	5·8	0·11
	Si–Si	3·03	3·9	0·13

of course not practicable to produce a simulation of the data from 'first principles' assuming a material of $MO_x(SiO_2)_{1-x}$.

P–O contributions have been included only in the 77S5 sample since, in the melt quenched samples, only 2·6 mol% P_2O_5 is present, whereas the 77S5 sol-gel sample contains 4 mol% P_2O_5. The results for the 77S5 sol-gel sample show two separate P–O distances corresponding to the separate P-bridging oxygens (P-BO), and the P-nonbridging oxygens (P-NBO). The correlation at 1·43 Å is assigned to the P-NBO bonds and has a coordination of ~3. The correlation at 1·58 Å is assigned to the P-BO bond and has a coordination of ~1. This agrees well with NMR data carried out by Novamin Technology,[20] which showed that 45S5 Bioglass contains mostly orthophosphate (Q^0) units, and that as the Si and P content increases, an increase in pyrophosphate (Q^1) units occurs.

5. Conclusions

The results of the first HEXRD study of bioactive glasses 45S5 (Bioglass) 55S5 60S5 and 77S5 are presented. It is shown that significant structural differences are observable in these samples as a function of composition and of preparation method. The main difference between preparation methods is that the sol-gel samples contain no Na and hence this can be seen clearly in the $T(r)$ functions as a missing feature at ~2·4 Å where the Na–O distance is found in the melt quenched $T(r)$'s. The effect of increasing amounts of Ca and Na on the underlying Si network can be seen in the O–Si–O pair correlation peak coordination, as the more Ca and Na present in the sample the more disrupted the Si network is. In the 77S5 sample two P–O correlations can be seen corresponding to P-BO and P-NBO and the relevant coordination numbers indicate a majority of pyrophosphate (Q^1) units.

Acknowledgments

References

1. Clark, A. E. & Hench, L. L. *J Biomed. Mater. Res.*, 1976, **10**, 161–74.
2. Clark, A. E, Pantano, C. G. & Hench, L. L. *J Am. Ceram. Soc.*, 1976, **59**, 37–9.
3. Ogino, M.,-Ohuchi, F. & Hench, L. L. *J Biomed. Mater. Res.*, 1980, **14**, 55.
4. Hench, L. L. *J. Am. Ceram. Soc.*, 1991, **74**, 1487–510.
5. Kim, C. Y., Clark, A. E. & Hench, L. L. *J Biomed. Mater. Res.*, 1992 **26**, 1147.
6. Hench, L. L. In: *Bioceramics, vol. 7, Proc. 7th Int. Symp. on Ceramics in Medicine*, Eds O. H. Andersson, R. P. Happonen & A. Uli-Urpo, Butterworth-Heinemann, Oxford, 1994, p. 3.
7. See www.novabone.com and www.novamin.com for commercial details.
8. Warren B. E. *X-ray Diffraction*, Dover Publications, New York, 1990.
9. Cole, J. M., van Eck, E. R. H., Mountjoy, G., Anderson, R., Brennan, T., Bushnell-Wye, G., Newport, R. J. & Saunders G. A. *J. Phys.: Condens. Matter.*, 2001, **13**, 4105.
10. Blackman, R. B. & Tukey, J. W. Particular Pairs of Windows. In *The Measurement of Power Spectra From the Point of View of Communications Engineering*. Dover, New York, 1959.
11. Gaskell, P. H. *Materials Science and Technology* vol 9, Ed. J. Zrzycky, VCH, Weinhaim, p 175, 1991.
12. Pickup, D. M., Mountjoy, G., Roberts, M. A., Wallidge, G. W., Newport, R. J. & Smith, M. E. *J. Phys.: Condens. Matter.*, 2000 **12** 3521.
13. Skipper, L. J., Sowrey, F. E., Pickup, D. M., Drake, K. O., Smith, M. E., Saravanapavan, P., Hench, L. L. & Newport, R. J. *J. Mater. Chem.*, 2005, **15**, 2369–2374.
14. Du, J. & Cormack A. N. *J Non. Cryst. Solids.*, 2004, **349**, 66–79.
15. Hoppe, U., Walter, G., Barz, A., Stachel D., & Hannon A. C. *J. Phys.: Condens. Matter.*, 1998, **10**, 261–270.
16. Gaskell, P. H., Eckersley, M. C., Barnes, A. C. & Chieux, P. *Nature*, 1991, **350**, 675.
17. Mead, R. N. & Mountjoy, G. *J Phys: Chem. B*, 2006, **110**, 14273–14278.
18. Wright, A. C. *Experimental Techniques of Glass Science*, Eds C. J. Simmons & O. H. El-Bayoumi, American Ceramic Society, Ohio, 1993, p. 205–314.
19. Pant, A. K. *Acta Crystallogr, B: Struct. Sci.*, 1968, **24**, 1077.
20. Greenspan, D. Private communication, Novamin Technology Inc., 13709 Progress Blvd., suite #23 Alachua, FL 32615, USA. Data to be published.